

# Preliminary Surface Pressure Measurements of Transitional, Hypersonic Shock Boundary Layer Interactions

Frank K. Lu\* and Kenneth A. Pistone†

University of Texas at Arlington, Arlington, Texas 76019-0018

**A laminar boundary layer at Mach 8 in air under perfect gas conditions was subjected to a shock interaction generated by a sharp ramp of 10 or 20 deg. The Reynolds number of the interaction was 2.27 million. It was found that the interaction stretches over a large extent and the inviscid downstream pressure was not obtained within the test region. Moreover, it was found that surface pressure disturbances were damped out rapidly. Based on the surface pressure measurements, it is concluded that the shocks created were not strong enough to cause transition.**

## Nomenclature

$M$	= Mach number
$p$	= pressure
$Re$	= Reynolds number
rms	= root mean square
$x$	= streamwise location along test surface
$\sigma$	= standard deviation

## Subscripts

$init$	= value just before run
$o$	= stagnation conditions
$p$	= pressure
$ref$	= reference
$test$	= value during test
$tr$	= transition
$u$	= unit
$x$	= local
$\infty$	= incoming freestream conditions

## Introduction

**A**DEQUATE understanding of the interaction between a shock wave and a boundary layer is of utmost importance as flight moves into the hypersonic realm. A critical aspect in designing an airbreathing hypersonic vehicle is in the forebody compression region ahead of the engines. Such a region is expected to be substantially laminar throughout a wide range of flight conditions. Hence, should the possibility of transition induced by the compression arise, there will be drastic alteration of the aerothermodynamics. For example, both drag and heat transfer will increase. Moreover, existing supersonic literature suggests that such a

transition process is likely to be accompanied by boundary layer separation, with well-known, adverse consequences' such as increased unsteadiness besides increased drag and heat transfer. A similar concern also exists around control surfaces. These concerns have prompted a number of recent investigations in understanding hypersonic, laminar and turbulent, shock wave, boundary layer interactions.<sup>2-6</sup> For simplicity, these investigations generally make use of a sharp ramp placed on a flat surface to generate the interacting shock. Such a configuration serves as a basic model for understanding more complex interactions over actual surfaces.

The condition of the boundary layer approaching the compression ramp plays an important role in determining the behavior of the interaction. For example, laminar, shock, boundary layer interactions separate more easily than turbulent interactions. In many instances, laminar separation is accompanied by turbulent reattachment, so that transition and separation are intimately related. (Observations of such phenomena date back to early work by Chapman, et al.<sup>8</sup>) Thus, the disturbance that causes the separation may also be responsible for causing early transition.

Even though transition of a hypersonic boundary layer is affected by many parameters, only the shock strength is considered in the present investigation. Significant gaps exist in the literature concerning shock-induced transition in the hypersonic regime. Therefore, initial experiments at a low Reynolds number were thought necessary for gaining some understanding of the process. These studies will then be followed by a systematic Reynolds number investigation. The current study is the first phase of a program to further the understanding of hypersonic transitional interactions. This paper reports preliminary surface pressure measurements of a ramp placed in a Mach 8, perfect gas flow. A laminar boundary layer developed over a sharp-edged flat plate and the Reynolds number at the ramp hingeline from the flat-plate leading edge was

\*Associate Professor and Director, Aerodynamics Research Center, Mechanical and Aerospace Engineering Department. Associate Fellow AIAA.

†Graduate Research Assistant, Aerodynamics Research Center, Mechanical and Aerospace Engineering Department. Student Member AIAA.

Copyright © 1996 by the American Institute of Aeronautics and Astronautics, Inc. All rights reserved.

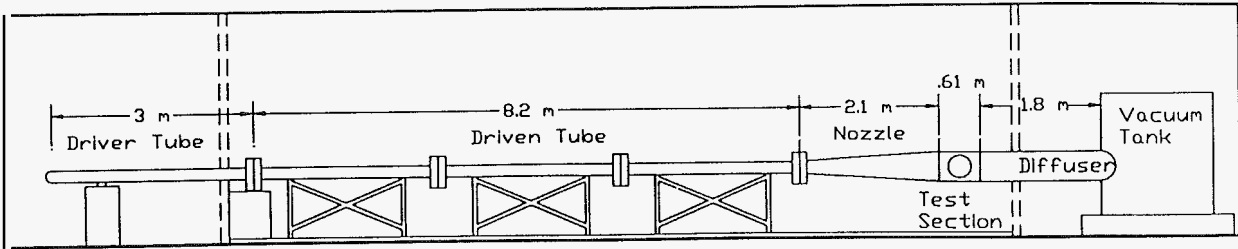


Figure 1: Schematic of shock tunnel.

2.27 million. It was found that surface pressure disturbances generated by ramps with angles as large as 20 deg were rapidly damped. Based on pressure measurements, these interactions were found to be too weak to induce transition.

### Experimental Methods

#### Test Facility

The experiments were performed at the University of Texas at Arlington's shock tunnel facility. A detailed description of the tunnel is given in Ref. 9 and only a brief description is given below. The reflected shock tunnel is of conventional design and consists of a driver connected to a plenum section, a driven tube, a nozzle, a test section, a diffuser, and a vacuum tank as shown in the schematic of Fig. 1. The driver section is 3 m (10 ft) long and it has a 14.24 cm (6 in.) diameter bore. The plenum section separates the driver from the driven tube by using two grooved steel diaphragms. Each has a rupturing pressure of approximately 15 MPa (2200 psi). Using two diaphragms allows a repeatable driver tube pressure of 24 MPa (3500 psi) to be obtained. The driven tube consists of three segments which total 8.22 m (27 ft) long and it has the same bore as that of the driver. It was operated at a pressure of 280 kPa (40 psi).

A thin diaphragm of aluminum foil was inserted in the throat of the nozzle to separate the driven tube from the nozzle section. The shock tunnel has a conical nozzle with a 7.5 deg half-angle expansion. The conical nozzle provided an acceptably uniform flow. Previous pitot surveys taken 0.33 m (13 in.) from the leading edge of the flat-plate test model showed that the inviscid core of the test gas was about 0.17 m (6.7 in.) in diameter. Connected to the nozzle is a 53.6 cm (21 in.) long test section of a semi free-jet design with a 44 cm (17.3 in.) diameter. A diffuser followed the test section and dumped the gas into a 4.25 m<sup>3</sup> (150 ft<sup>3</sup>) cylindrical vacuum tank which was outfitted with

a valve that vented the tunnel when the pressure rose above 100 kPa (15 psi).

#### Model

The model consisted of a flat plate and a ramp. The flat plate was 203 mm (8 in.) wide and 0.96 m (37.75 in.) long. The plate was mounted 50 mm (2 in.) below the centerline of the shock tunnel's test section. Side fencing was also built into the underside of the flat plate to prevent crossflows. The flat plate was longer than the test section and it protruded into the nozzle and diffuser sections of the tunnel. The upper surface of the flat plate consisted of a nose piece with a sharp leading edge, followed by four 203 mm (8 in.) square sections. The first section was replaced by the ramp as shown in Fig. 2.

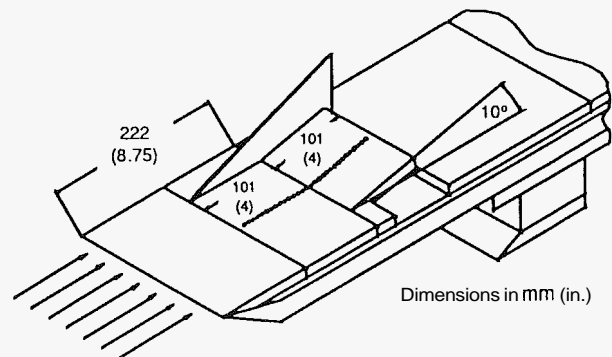


Figure 2: Schematic of test model (one side fence shown).

The instrumented flat plate, which was 101.6 mm (4 in.) long, was attached in front of a ramp of the same length, but with a width of 127 mm (5 in.). Pressure taps were drilled at 6.35 mm (0.25 in.) intervals along the instrumented flat plate and ramp. The taps were

3.18 mm (0.125 in.) off the centerline of the test plate. The hinge line of the ramp was positioned 222.3 mm (8.75 in.) behind the sharp leading edge of the flat plate. The first of the 30 pressure taps was 92.1 mm (3.75 in.) in front of the hinge line and the last was 92.1 mm (3.75 in.) behind. It was subsequently found that the ramp was not long enough to capture the inviscid pressure downstream. Two ramps, at 10 and 20 deg respectively, were used. Side fences were employed to ensure two dimensionality. The side fences extended from 101.6 mm (4 in.) in front of the hinge line to that same distance behind with the height of the side fencing at the rear of the ramp being 88.9 mm (3.5 in.) above the surface of the flat plate. The fences were 7.35 mm (0.25 in.) thick. Their tops were beveled outward at 60 deg and their sharp leading edges were set at 41 deg to the incoming flow.

No comprehensive survey of the transition zone was conducted in the present study. Instead, the length to the end of the transition zone was obtained from

$$x_{tr} \text{ (meters)} = \frac{149 + 536(M_\infty - 3)^{1.5}}{Re_u^{0.6}} \quad (1)$$

where  $Re$ , is the unit Reynolds number per meter. Equation (1) is adapted from an empirical formula developed in Ref. 12 for the transition length of a boundary layer developing over a flat plate with a sharp leading edge. For a recent study on the transition zone, see Ref. 7. From Eq. (1), the transition length based on an unit Reynolds number  $Re = 10.2 \times 10^6$  per m and a Mach number  $M_\infty = 8$  over a flat plate with a sharp leading edge was 383 mm (15.07 in.). The transition Reynolds number was therefore 3.9 million. To ensure that the shock interacted with a laminar flow, the ramp was located ahead of the transition at 222.3 mm (8.75 in.) from the sharp leading edge of the flat plate. The Reynolds number at the ramp was thus  $Re = 2.27$  million. Moreover, based on Inger's analysis,<sup>13</sup> the present Mach and Reynolds numbers would yield incipient separation due to a shock with a pressure ratio of 1.318. In other words, it is expected that the ramps used would induce separation. Alternatively, based on previous correlations,<sup>14,15</sup> the ramp angle for incipient separation under the present conditions is of the order of 5 to 7 deg.

#### Measurement Techniques

A LeCroy Model 1434A CAMAC high-speed data acquisition system with two Model 6810 recorders was used. These two modules allowed eight channels of 12-bit data to be gathered simultaneously at a sampling rate of one million/s. All channels were triggered simultaneously. The transducers were powered by a Tektronix Model CPS250 15 V DC power supply. The waveform recorders were controlled by a LeCroy Model 8901A interface module which linked the data acquisition system to a personal computer via two National

Instruments Model GPIB-110 bus extenders.

Of the eight channels, one was used for obtaining the stagnation pressure measured at the downstream end of the driven tube. The signal from this channel was also used to trigger the data acquisition system. A second channel was used to obtain a reference pressure  $p_\infty$  measured on the test surface ahead of the interaction. This reference pressure was used to normalize the interaction pressures measured by the remaining six channels. The limited number of channels meant that a complete pressure distribution was obtained by a number of runs. The orifices not in use by pressure transducers were plugged with flush-mounted brass rods.

Kulite Model XCS-093-5A pressure transducers were the instrumentation used throughout the experiments. These transducers are rated from 0–35 kPa (0–5 psia) with a three times over range. The pressure transducers have a sensing surface of 0.97 mm (0.038 in.) in diameter and an outside diameter of 2.36 mm (0.093 in.). These transducers were fitted with type B screens which afforded more protection than the M screens that are normally provided with the XCS-093 transducers. The transducers were flush-mounted perpendicularly with the test surface using a machinist's block so the test surface was smooth to  $\pm 0.064$  mm ( $\pm 0.0025$  in.).

Static calibrations were used to determine the transducers' sensitivities prior to each experiment. The calibrations were necessitated by drift and hysteresis of the transducers. To minimize the effect of drift, the pressure transducers were calibrated against an MKS Baratron Model 127A vacuum gauge while the test section of the shock tunnel was being evacuated. The Baratron vacuum gauge is a widely used secondary standard and is accurate to  $\pm 7$  kPa ( $\pm 0.001$  psia). Applying a linear least squares fit to the calibration data provided sensitivities for the transducers which were fairly consistent and matched well with the manufacturer's specifications. Approximately 30 minutes would elapse between transducer calibration and a run. During this time, significant zero shift occurred. To overcome the shift problem, a reading from the vacuum gauge was taken just prior to firing the tunnel and compared to the calibration data so that the offset could be determined. Thermal zero shift and thermal sensitivity problems that are encountered with piezoresistive transducers were not a factor due to the short run times of the tests.

#### Test Conditions

The performance of the shock tunnel was determined using inviscid perfect gas relations<sup>16</sup> with stagnation conditions determined from calibrations in Ref. 10. The driver tube pressure  $p_4$  was maintained at 24 MPa (3500 psia)  $\pm 4$  percent with the plenum section charged to approximately 12 MPa (1750 psia). The driven tube pressure  $p_1$  was 280 kPa (40 psia)  $\pm 1$  percent. The test section, diffuser, and vacuum tank were evacuated to

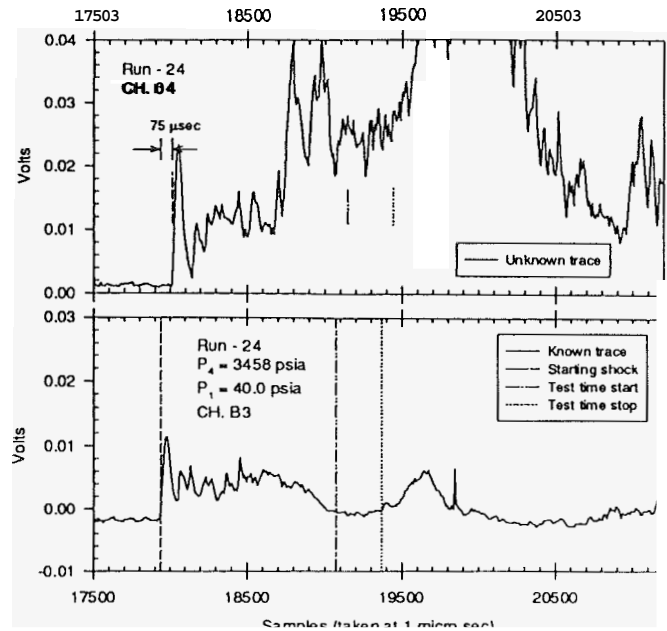


Figure 4: Determining test window of an unknown pressure trace by using the test window of a known trace.

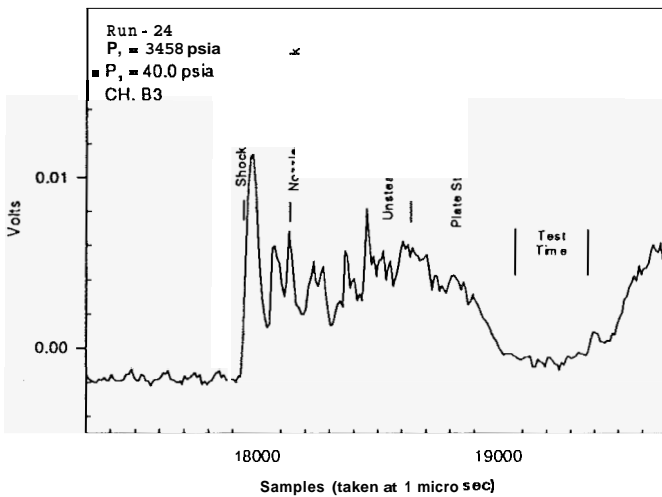


Figure 3: Example of filtered output from a surface mounted transducer.

### Test Time

The useful test time was determined by examining the pressure traces. First, the raw data were digitally filtered to 100 kHz. An example of the filtered output

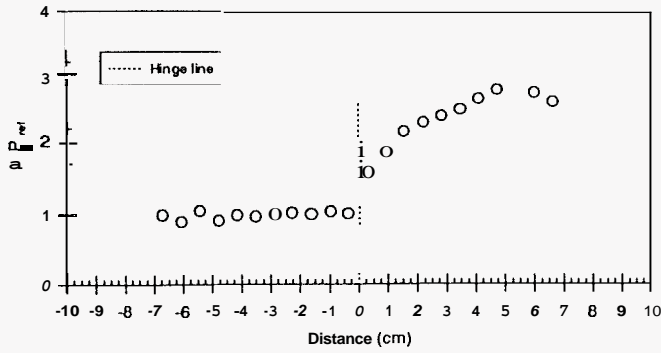
from a surface mounted transducer is shown in Fig. 3. The figure shows a substantial starting process followed by the useful test time of shorter duration and then by flow breakdown. It should be noted that the present tests were not performed with the tailored mode of operation to simplify test procedures. But this was achieved with a shorter available test time. Whereas Fig. 3 shows a clearly discernible test time, detection of the test time when the flow encounters a disturbance becomes challenging due to the unrecognizable form of the pressure trace. The test time of a pressure trace can be determined if the test time from another transducer is known. This procedure is shown in Fig. 4.

The reference pressure transducer located ahead of the interaction on the instrumented flat plate provided the means to always distinguish the test time at a point. The starting point of a pressure trace was determined for the reference transducer and for the transducer with the unknown test window. In this example, a lag of 75  $\mu$ s occurred. The unknown test window thus lagged by the same amount and is indicated in the figure. The test times encountered in this investigation ranged from 200 to 400  $\mu$ s. Further discussion of experimental techniques can be found in Ref. 17.

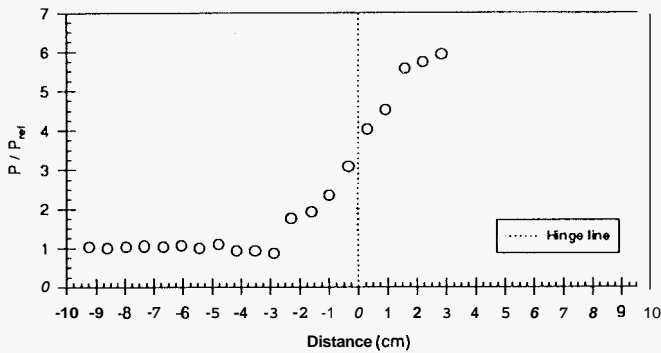
### Results and Discussion

#### Mean Surface Pressure

The mean surface pressure distributions of the ramp



a. 10 deg ramp.



b. 20 deg ramp.

Figure 5: Mean surface pressure.

induced interaction are shown in Fig. 5. The influence of the 10 deg ramp on the flow is felt about 10 mm upstream of the hinge line.

The pressure rises across the hinge line until 40 mm downstream where the pressure level plateaus at a value of  $p/p_{ref}$  of about 3. The pressure starts to decrease slightly from 50 mm past the hinge line. The measured pressure ratio did not reach the inviscid level of 5.75. Possible reasons for not achieving the full pressure recovery are tunnel wall interference and disturbances from flow expansion over the top of the ramp. A small number of tests was devoted to repeatability and two-dimensionality checks. The results are shown in Figs. 6 and 7. These figures show that repeatability and two-dimensionality is good.

Figure 5b shows the mean pressure distribution for the 20 deg ramp. The influence of the 20 deg ramp on the flow is felt 20–30 mm upstream of the hinge line. The pressure sharply rises near the hinge line until 10–30 mm downstream where the pressure level starts to plateau at  $p/p_{ref}$  of 6–7. However, similar to the 10 deg ramp, the pressure never reached the inviscid level

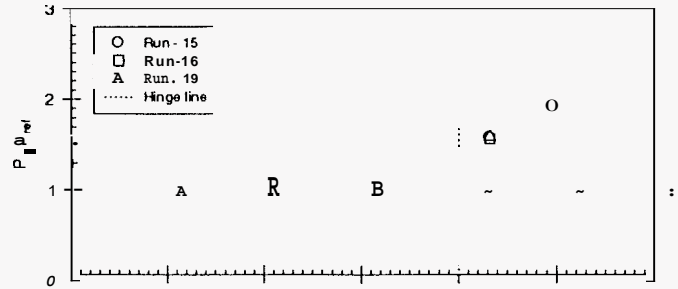


Figure 6: Repeatability tests for 10 deg ramp.

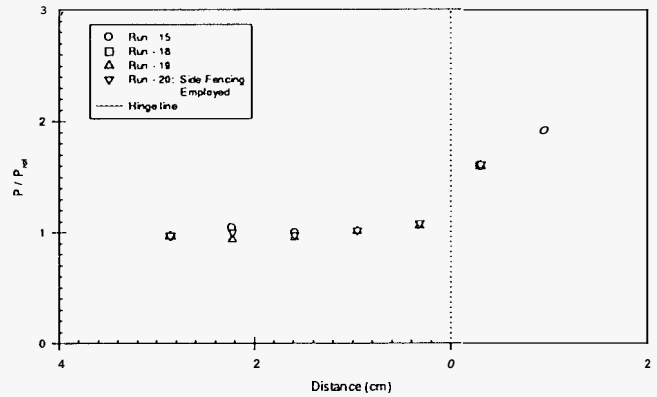


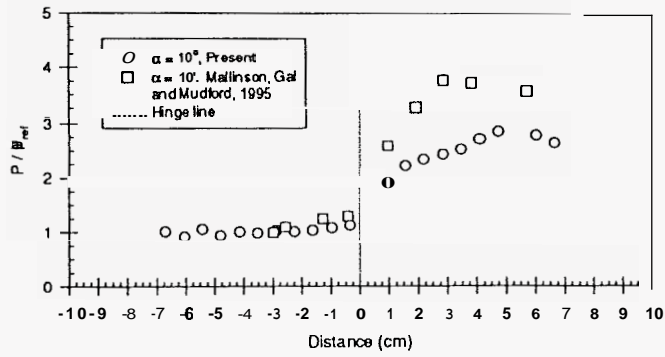
Figure 7: Two-dimensionality tests for 10 deg ramp.

downstream. In this case, the pressure ratio is 14.8.

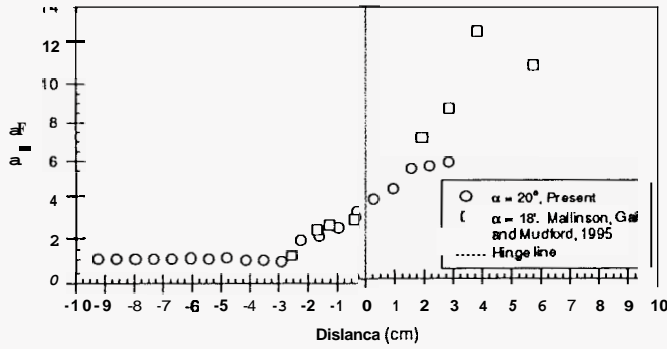
Nevertheless, the surface pressure distribution obtained by Mallinson et al.<sup>6</sup> exhibited the same phenomenon. This is shown in Fig. 8. Mallinson et al.<sup>6</sup> performed experiments similar to this investigation; however, their experiments were run under real gas conditions, at a unit Reynolds number of 3.22 million per meter, an incoming Mach number of 9.1 and a ramp angle of 10 or 18 deg. Figure 8a shows that, for the 10 deg ramp, the upstream influence of Mallinson et al.'s experiments was close to that obtained in the present investigation of about 10 mm. Their data did not achieve the downstream inviscid value. Similar observations can be made for their 18 deg ramp versus the present 20 deg ramp experiments, as shown in Fig. 8b. That is, the upstream influences were comparable whilst the downstream inviscid value was not obtained.

#### RMS Surface Pressure Data

The mean surface pressure distribution is not a sensitive indicator of transition whereas an increase in un-



a. 10 deg ramps.



b. Present 20 deg ramp and Mallinson et al.'s 18 deg ramp.

Figure 8: Comparison with Mallinson et al.

steadiness is likely to indicate turbulence. Therefore, in addition to the mean surface pressure, the data were processed to obtain an indication of the effect of the shock disturbance on the surface pressure fluctuations. This technique, unfortunately, cannot differentiate between surface pressure unsteadiness due to turbulence or from shock unsteadiness. Nevertheless, the hypothesis is that if the fluctuations remain at a high level after passing the shock, then it is likely that the boundary layer would have transitioned.

For each pressure trace, the rms obtained of the test window  $\sigma_{p_{test}}$  is normalized against the rms value of the transducer at the beginning of the run  $\sigma_{p_{init}}$ , to yield

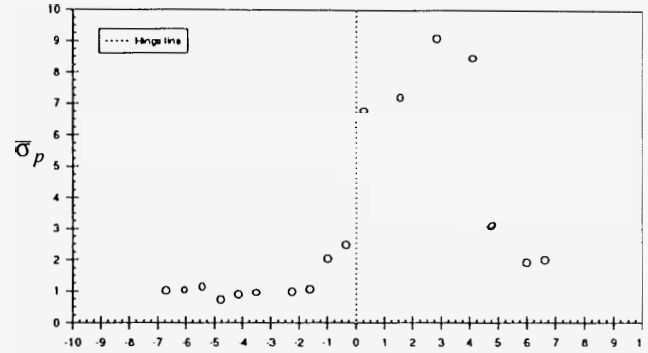
$$\sigma'_{p_{test}} = \sigma_{p_{test}} / \sigma_{p_{init}} \quad (2)$$

This procedure removes the effect of the transducer's background noise, since each transducer has a different noise content. Normalized rms distributions of pressure fluctuations are shown in Fig. 9. To determine the amplification of pressure fluctuations by the shock, the normalized fluctuation is compared against the normal-

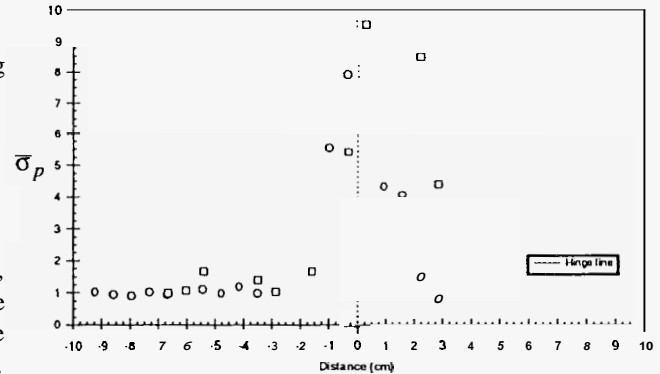
ized fluctuation of the reference transducer, namely,

$$\bar{\sigma}_p = \sigma'_{p_{test}} / \sigma_{p_{\infty}} \quad (3)$$

The normalized rms distribution for the 10 deg ramp is shown in Fig. 9a. The figure shows that the influence of occurs 10-20 mm upstream of the hinge line. The normalized fluctuations rise sharply to a level of about 9 at approximately 30 mm downstream of the hinge line. The fluctuations dampen almost to their starting levels 60-70 mm downstream of the hinge line.



a. 10 deg ramp.



b. 20 deg ramp.

Figure 9: Surface pressure fluctuations.

The normalized rms distribution for the 20 deg ramp is shown in Fig. 9b for two sets of tests. In both tests, the upstream influence occurs about 40 mm ahead of the hingeline. The normalized fluctuations rise sharply to a value of about 10 around the hingeline. The fluctuations dampen back to their starting levels 20-40 mm downstream of the hinge line.

The surface pressure of a pure laminar flow would not exhibit any pressure fluctuations. In other words, the normalized rms value  $\bar{\sigma}_p$  is unity. A flow that has transitioned to a turbulent one would be characterized by large fluctuations, yielding a normalized rms value

transitioned to a turbulent one would be characterized by large fluctuations, yielding a normalized rms value above unity. The present experiments show that the shock wave induces large fluctuations in pressure to occur, with the fluctuations peaking at the hingeline or just downstream of it. The disturbances appear to be damped out rapidly. It is conjectured that the lack of any further significant fluctuations is an indication that the disturbance was not strong enough to trigger early transition. However, complete validation of whether early transition occurred based on surface pressure measurements was not feasible because the present ramps were not long enough.

### Conclusions

Experiments were carried out to study the effects that a ramp-induced shock would have upon a laminar boundary layer in hypersonic flow. The aim of the study was to determine both the size and the location of the disturbance necessary to cause transition. The interactions were examined by surface pressure measurements and an analysis of pressure fluctuations. The conclusions from this investigation are summarized as follows:

1. The shock, boundary layer interaction created using both the 10 and 20 deg ramps did not cause the flow to transition ahead of the flat plate transition location. This conclusion was based on the dampening of pressure fluctuations downstream of the ramp hingeline.
2. The upstream influence was evident in both the mean and rms surface pressure distribution. The larger disturbance generated by the 20 deg ramp yielded a larger upstream influence. Pressure levels did not meet expected values behind an oblique shock. A possibility exists that these values cannot be reached due to limitations of the shock tunnel. The shock tunnels inviscid core of test gas may not be large enough to contain a ramp of sufficient length to meet these expected values.

In addition to the above tests, there are ongoing plans to perform heat transfer tests which is expected to be a sensitive indicator of transitional phenomena. Reynolds number variation, such as moving the ramp further back, is also contemplated.

### Acknowledgements

This study was conducted as part of the NASA/UTA Center for Hypersonic Research under Grant No. NAGW 3714. Additional funding was provided by Lockheed-Martin Tactical Aircraft Systems through Purchase Order No. 4286428, "Development of Hypersonic Technologies."

### References

- <sup>1</sup>Delery, J. and Marvin, J. G., "Shock-Wave Boundary Layer Interactions," AGARD-AG-280, 1986.
- <sup>2</sup>Heffner, K. S., Chpoun, A. and Lengrand, J. C., "Experimental Study of Transitional Axisymmetric Shock-Boundary Layer Interactions at Mach 5," AIAA Paper 93-3131, 1993.
- <sup>3</sup>Simeonides, G., Haase, W. and Manna, M., "Experimental, Analytical, and Computational Methods Applied to Hypersonic Compression Ramp Flows," *AIAA Journal*, Vol. 32, No. 2, 1994, pp. 301-310.
- <sup>4</sup>de Luca, L., Cardone, G., Aymer de la Chevalerie, D. and Fonteneau, A., "Viscous Interaction Phenomena in Hypersonic Wedge Flow," *AIAA Journal*, Vol. 33, No. 12, 1995, pp. 2293-2298.
- <sup>5</sup>Holden, M. S. and Chadwick, K. M., "Studies of Laminar, Transitional, and Turbulent Hypersonic Flows Over Curved Compression Surfaces," AIAA Paper 95-0093, 1995.
- <sup>6</sup>Mallinson, S. G., Gai, S. L. and Mudford, N. R., "High Enthalpy, Hypersonic Compression Corner Flow," AIAA Paper 95-0155, 1995.
- <sup>7</sup>Chapman, D. R., Kuehn, D. M. and Larson, H. K., "Investigation of Separated Flow in Supersonic and Subsonic Streams with Emphasis on the Effects of Transition," NACA Report No. 1356, 1958.
- <sup>8</sup>Lu, F. K., "Initial Operation of the UTA Shock Tunnel," AIAA Paper 92-0331, 1992.
- <sup>9</sup>Chung, K.-M., "Shock Impingement near Mild Hypersonic Expansion Corners," Ph.D. Dissertation, University of Texas at Arlington, December 1992.
- <sup>10</sup>Chung, K.-M. and Lu, F. K., "Hypersonic Turbulent Expansion-Corner Flow with Shock Impingement," *Journal of Propulsion*, Vol. 11, No. 3, 1995, pp. 441-447.
- <sup>11</sup>Deem, R. E. and Murphy, J. S., "Flat Plate Boundary Layer Transition at Hypersonic Speeds," AIAA Paper 65-0128, 1965.
- <sup>12</sup>Kimmel, R. L., "The Effect of Pressure Gradient on Transition Zone Length in Hypersonic Boundary Layers," Report WL-TR-94-3012, Wright Laboratory, Wright-Patterson Air Force Base, Ohio; also, *Transitional and Turbulent Compressible Flows*, FED Vol. 151, ASME, pp. 117-127.
- <sup>13</sup>Inger, G. R., "Similitude Properties of High-speed Laminar and Turbulent Boundary-Layer Incipient Separation," *AIAA Journal*, Vol. 15, No. 5, 1977, pp. 619-623.
- <sup>14</sup>Holden, M. S., "Boundary-Layer Displacement and Leading-Edge Bluntness Effects on Attached and Separated Laminar Boundary Layers in a Compression Corner. Part II: Experimental Study," *AIAA Journal*, Vol. 9, No. 1, 1971, pp. 84-93.
- <sup>15</sup>Bloy, A. W. and Georgeff, M. P., "The Hypersonic Laminar Boundary Layer near Sharp Compression and Expansion Corners," *Journal of Fluid Mechanics*, Vol. 63, 1974, pp. 431-447.
- <sup>16</sup>Stuessy, W. S., Lu, F. K., Wilson, D. R. and Murtagudde, R. G., "Development of the UTA Hypersonic Shock Tunnel," AIAA Paper 90-0080, 1990.
- <sup>17</sup>Pistone, K. A., "Surface Pressure Measurements of Hypersonic Transitional Flow Across a Ramp," M.S.M.E. Thesis, University of Texas at Arlington, May 1996.